

Minimizing End-to-End Delay: A Novel Routing Metric for Multi-Radio Wireless Mesh Networks

Hongkun Li, Yu Cheng, Chi Zhou
 Department of Electrical and
 Computer Engineering
 Illinois Institute of Technology
 {hli55, cheng, zhou}@iit.edu

Weihua Zhuang
 Department of Electrical and
 Computer Engineering
 University of Waterloo
 wzhuang@uwaterloo.ca

Abstract—This paper studies how to select a path with the minimum cost in terms of expected end-to-end delay (EED) in a multi-radio wireless mesh network. Different from the previous efforts, the new EED metric takes the queuing delay into account, since the end-to-end delay consists of not only the transmission delay over the wireless links but also the queuing delay in the buffer. In addition to minimizing the end-to-end delay, the EED metric implies the concept of load balancing. We develop EED-based routing protocols for both single-channel and multi-channel wireless mesh networks. In particular for the multi-radio multi-channel case, we develop a generic iterative approach to calculate a multi-radio achievable bandwidth (MRAB) for a path, taking the impacts of inter/intra-flow interference and space/channel diversity into account. The MRAB is then integrated with EED to form the metric of weighted end-to-end delay (WEED). As a byproduct of MRAB, a channel diversity coefficient can be defined to quantitatively represent the channel diversity along a given path. Both numerical analysis and simulation studies are presented to validate the performance of the routing protocol based on the EED/WEED metric, with comparison to some well-known routing metrics.

I. INTRODUCTION

Routing in wireless mesh networks has been a hot research area in recent years, with the objective to achieve as high throughput as possible over the network. The main methodology adopted by most of the existing work is selecting path based on interference-aware or load-balancing routing metrics to reduce network-wide channel contentions. It has been revealed that the capacity of a single-radio multi-hop wireless network can not scale up with the network size, due to the co-channel interference [1]–[3]. The multi-radio multi-channel connection has been widely considered as an efficient approach to increase the wireless network capacity [8]. Design of efficient routing schemes for multi-radio multi-channel wireless mesh network is much more challenging compared to the single-channel case.

Many popular multimedia applications, e.g., voice over IP, IPTV, and on-line gaming, have strict delay requirement. In this paper, we aim at designing a routing metric to minimize the end-to-end delay, considering not only the transmission delay at the medium access control (MAC) layer, but also the queuing delay at the network layer. Most of the previous studies focus only on the transmission delay of the packet

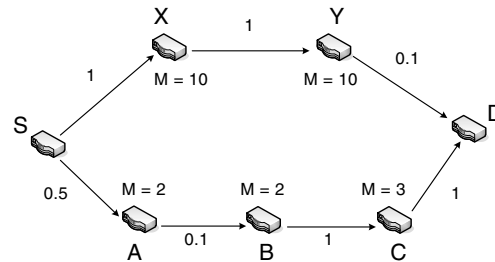


Fig. 1. The impact of queuing delay on path selection.

being served at the MAC layer [13], [15], while in many cases the queuing delay takes a significant portion of the total delay over a hop. The delay through a node, which has many packets in queue but short transmission time, could be larger than through the one, which has less packets in the queue but longer transmission delay.

We here use an example, as illustrated in Fig. 1 to emphasize the impact of network-layer queuing delay on routing. The number annotating each link is the success probability for a transmission over the link, denoted as p_{suc} , which means on average it takes $1/p_{suc}$ transmission trails to successfully deliver a packet. The number M denotes the number of packets in the network-layer queue, waiting to be served by the MAC layer. Suppose that the bandwidth of each link is 11Mbit/s and the packet length is 1100bytes; it gives a transmission time of 0.8ms. If the queue delay is not included, routing based on the expected transmission time (ETT) would prefer the path S-X-Y-D (9.6ms) over the path S-A-B-C-D (11.2ms). Nevertheless, the path S-A-B-C-D would be the better one with the queuing delay taken into account. In this case, the end-to-end delay over S-X-Y-D is 97.6ms, but only 24 ms over S-A-B-C-D. In this example, the delay values ignore the backoff overhead, which will be considered in our routing metric design.

The newly proposed routing metric of end-to-end delay (EED) in fact exploits the cross-layer design: each node needs to not only monitor the transmission failure probability at the MAC layer to estimate the MAC transmission delay, but also count the number of packets waiting in the network-layer buffer to estimate the queuing delay. The EED metric also implies the concept of load-balancing. The path with

This work was supported in part by NSF grant CNS-0832093.

minimum EED normally passes through the links with less packets in the queue, and thus balances the traffic off those congested links. Moreover, counting the number of packets in the buffer is a convenient implementation; most of the existing load-balancing routing schemes require the traffic information available, which is usually not easy to obtain in practice [16].

In addition to the transmission delay and queuing delay at each hop, the end-to-end delay over a multi-hop wireless network is particularly impacted by the interferences among different hops, which can be classified into inter-flow and intra-flow interference [23]. In this paper, we further propose a path metric called *multi-radio achievable bandwidth* (MRAB) to accurately capture the impacts of inter/intra-flow interferences and space/channel diversity along a path. We consider a practical scenario that an end-to-end path may consist of both multi-radio hops and single-radio hops, where different channels do not interfere with each other but interferences exist within the same channel. We particularly develop a sub-path based iterative approach to model the complex interactions among inter-flow interference, intra-flow interference, and simultaneous transmission due to space and channel diversity. The MRAB is then integrated with EED to form the metric of weighted end-to-end delay (WEED). As a byproduct of MRAB, a channel diversity coefficient can be defined to quantitatively represent the channel diversity along a given path. We evaluate the performance of the WEED based routing protocol via numerical analysis and ns2 simulations, with comparison to some popular metrics, under both single and multiple channel cases. It is confirmed that the EED/WEED metric consistently yields better performance.

The remainder of this paper is organized as follows: Section II reviews more related work. Section III derives the routing metric of EED. Section IV presents the algorithm to compute the MRAB, which captures the interaction between the inter- and intra-flow interferences. The MRAB metric is integrated with the EED metric to form the WEED metric for routing over the multi-radio mesh networks. The routing protocol is described in Section V. Section VI presents some numerical analysis and simulation studies to validate the routing performance based on the EED/WEED metric, with comparison to some well-known routing metrics. Section VII gives the concluding remarks.

II. RELATED WORK

The routing metric plays a critical role in a routing protocol. The studies in [8], [16], [17] design routing metrics for load-balancing in a multi-hop wireless network. The routing metrics however require the real-time traffic information. To exploit the space diversity, the link conflict graph is normally applied to model the interference among different hops [18], and the *interference clique transmission time* is proposed as a routing metric in [20]. However, the conflict graph based approaches normally induce large computation overhead in searching for the maximal independent sets or cliques, and are not suitable for dynamic distributed routing protocols. De Couto *et al.* propose the metric of *expected transmission*

count (ETX) [21] to describe the channel contention level experienced by a wireless link, which works well in a homogeneous single-radio environment. However, ETX is not capable of describing the complex scenarios in a multi-radio wireless mesh network, normally involving inter-/intra-flow interferences and different rate/interference/topology profiles over different channels. mETX and ENT [6] are proposed to enhance ETX by considering the variable link reliability. The ETOP metric enhances ETX by incorporating the impact of link positions [5].

A bandwidth-aware routing with QoS requirement is proposed in [26]. The link metric of *expected transmission time* (ETT) and the associated path metric of weighted cumulative ETT (WCETT) are proposed in [13] for multi-channel mesh networks, which try to enhance the ETX by counting the heterogeneous channel rate and intra-flow interference, but the inter-flow interference is still not considered. Furthermore, when calculating the intra-flow interference, WCETT always takes all links into account and overlooks the situation that two links far away enough can transmit packets simultaneously. The metric of interference and channel switching (MIC) [15] incorporates both inter-flow and intra-flow interference, whereas it only contains the number of interfering nodes rather than the total amount of interference on these nodes for the inter-flow interference. In [25], we propose a metric of *multi-hop effective bandwidth* (MHEB) to compute the usable bandwidth when both inter- and intra-flow interferences are present. However, the MHEB metric just uses a simple weighted average to combine the inter- and intra-flow interferences. In this paper, the MRAB is based on MHEB, but use a more accurate approach to capture the complex interplay between the two types of interferences.

III. END-TO-END DELAY METRIC

The end-to-end delay over a path is the summation of delays experienced by all the hops along the path. For convenience, we also use EED to denote the delay metric at each link. The meaning of EED will be clear in the context. In order to compute the EED metric over a wireless channel, each node needs to monitor the number of packets buffered at the network layer waiting for MAC layer service, as well as measuring the transmission failure probability at the MAC layer. The *transmission failure probability* is the probability that a MAC-layer transmission fails due to either collisions or bad channel quality. While counting the number of packets in the queue is straightforward, we will discuss how to measure the transmission failure probability over a link in Section V. The EED over a link i , say between node n_i and n_{i+1} , consists of the queuing delay and transmission delay as

$$EED_i = E [\text{queuing delay} + \text{transmission delay}]. \quad (1)$$

The *transmission delay* can also be interpreted as the packet service time, which is defined as the period from the instant that a packet begins to be serviced by the MAC layer to the instant that it is either successfully transmitted or dropped after a predefined number of retransmissions.

Suppose that the 802.11 distributed coordination function (DCF) MAC protocol is used, each transmission or retransmission includes protocol overhead due to the binary backoff mechanism [28]. Let p_i denote the transmission failure probability over link i , and assume it is stable through all the retransmissions of the packet. Also, let T_i denote the packet service time over link i , and K the maximum number of retransmissions. The average transmission delay

$$E[T_i] = \sum_{k=1}^{K+1} p_i^{k-1} (1-p_i)^{I\{k < K+1\}} \sum_{j=1}^k \left(E[W_j] + \frac{L}{B} \right) \quad (2)$$

where W_j denotes the contention window at the j th backoff stage, and L, B denote the packet length and link bandwidth, respectively. According to the 802.11 standard [7], [28], $W_j = 2^{j-1} W_{min}$ if ignoring the constraint of backoff stage, and $E[W_j] = \frac{W_j-1}{2}$. In (2), the indicator $I(A)$ is equal to 1 if A is true, which is incurred to include the case that a packet is dropped when the retransmission limit is reached. In addition, the MAC overhead due to acknowledgement is incorporated into the packet length L for convenience. After applying some manipulations over (2), we can get

$$E[T_i] = \frac{L}{B} \left[\frac{1-p_i^K}{1-p_i} \right] + E[\text{backoff time}] \quad (3)$$

with

$$\begin{aligned} E[\text{backoff time}] &= \sum_{k=1}^{K+1} p_i^{k-1} (1-p_i)^{I\{k < K+1\}} \sum_{j=1}^k E[W_j] \\ &= \frac{W_{min} [1 - (2p_i)^{K+1}]}{2(1-2p_i)} - \frac{1-p_i^K}{2(1-p_i)}. \end{aligned} \quad (4)$$

If there are M_i packets in the queue when a new packet reaches node n_i , the EED metric can be defined as

$$EED_i = (M_i + 1)E[T_i] \quad (5)$$

which means the total delay passing through the hop equals the MAC service time of those packets queuing ahead of the new packet plus the MAC service time of the new packet itself. Note that the EED value in (5) implies the memoryless property of the packet service time, as the head-of-line packet may only need to finish a residue packet service time when the new packet comes in. It is well-known that only an exponentially distributed services time has the memoryless property. It has been demonstrated in [30] that the MAC packet service time over a 802.11 DCF can indeed be approximated by an exponential random variable.

Consider an end-to-end path including H hops, the EED metric for the path is defined as

$$EED = \sum_{i=1}^H EED_i. \quad (6)$$

We would like to emphasize that the EED given in (6) does not consider the effect of co-channel interference in the multi-hop wireless networks, which assumes that all the packets can

continuously go through the path hop-by-hop. However, in a multi-hop wireless network, if two links working over the same channel are located close, when one link is in transmission, the MAC protocol will freeze the other link. Such channel freezing can be due to either intra-flow transmissions or inter-flow transmissions, which results in extra delays in addition to the basic EED as shown in (6). In the following section, we will discuss how to extend the basic EED with the co-channel interferences taken into account.

IV. ACHIEVABLE BANDWIDTH OVER A MULTI-RADIO MULTI-CHANNEL PATH

In this section, we will develop an algorithm to compute the achievable bandwidth along a multi-radio multi-channel path, termed as *multi-radio achievable bandwidth*, by capturing the complex interplay between inter-flow and intra-flow interferences. The end-to-end delay over a multi-radio multi-channel path can be described more accurately by incorporating the MRAB metric into the EED computation to form a new metric WEED. A side-effect benefit of MRAB analysis is that a *channel diversity coefficient* can be defined to quantify the resource consumption along a multi-radio multi-channel path.

A. Multi-Radio System

We consider a wireless mesh network, where each node is equipped with one or more radio interfaces. The interfaces assigned with different channels, located either in the same node or in different nodes, can be active simultaneously. Thus, the network throughput could be significantly improved compared with single-radio system [8]. The interfaces working on different channels would form distinct interference topologies. Channel assignment [10] plays an critical role in determining the interference topology, and then impacts on system performance. The channel assignment itself is a challenging research topic, which is out of the scope of this paper. We assume that the channel assignment for each node is given. All the nodes are stationary, and any one can be used as a router. We define the transmission range of a node as *one hop*, while the interference range is $r (\geq 2)$ hops. We consider that the WMN operates over the IEEE 802.11 based MAC, and assume that the routing control information exchanged among neighbor nodes is error free.

We adopt the physical model presented in [18] to describe the interference among different hops. Such an interference model indicates that a transmission from node u to v is successful if the signal to interference and noise ratio (SINR) at receiver v is above the pre-determined threshold γ , i.e.,

$$\frac{P_v(u)}{N + \sum_{k \in v'} P_v(k)} \geq \gamma \quad (7)$$

where N denotes the background noise, $P_v(u)$ the received power at node v from node u , v' the set of nodes located in interference range of v , and $P_v(k)$ the interference power from an interfering node k .

B. Multi-Radio Achievable Bandwidth

1) *Inter-flow interference*: we first compute the *achievable bandwidth under the inter-flow interference* (ABITF). Every node can monitor the received power to infer the magnitude of the inter-flow interference around its neighborhood. Based on the interference model (7), the SINR threshold implicitly denotes the maximum interference a node could tolerate to process a successful communication. We define the *interference degree ratio* $IDR_i(uv)$ for link i between u and v as:

$$IDR_i(uv) = \frac{\sum_{k \in v'} P_v(k)}{P_{max}}. \quad (8)$$

The ratio reflects the utilization of the channel assigned to link i . P_{max} is the maximum tolerable interference power at receiver and can be calculated by (7). $\sum_{k \in v'} P_v(k)$ is sum of undesired powers at node v from other transmissions. Note that if there is no interference, the IDR is 0, implying that entire bandwidth of this channel is available for link i . On the contrary, an IDR of 1 will indicate that the channel has been fully occupied by other links, and no additional bandwidth can be allocated for link i until the ratio becomes less than 1. Based on this definition, we evaluate the ABITF at link i as

$$ABITF_i = \frac{(1 - IDR_i)B_i}{ETX_i} \quad (9)$$

where B_i denotes the physical bandwidth of link i , and ETX_i [21] denotes the *expected transmission attempts* to achieve a successful transmission over link i . The value $(1 - IDR_i) * B_i$ indicates the available bandwidth for a transmission under the inter-flow interference. The physical meaning of (9) can be interpreted as: given the transmission failure probability p_i , a successful transmission needs ETX_i attempts in average; the bandwidth is effectively used for only one of the ETX_i transmission attempts.

2) *Intra-flow interference*: There exists intra-flow interference if two links belonging to the same path work on the same channel and are located within each other's interference range, i.e. within r (≥ 2) hops. We define a new concept of *sub-path* spanning $r + 2$ hops, based on the observation that a link will potentially interfere with another link at most $r + 2$ hops away. A sub-path with $r = 2$ is illustrated in Fig.2. In general, a H -hop path contains $H - r - 1$ sub-paths.

Under the impact of intra-flow interference, a sub-path is equivalent to a virtual link. The reason is that a new packet can enter a sub-path only after the previous one leaves. The achievable bandwidth over a sub-path can be iteratively obtained from the achievable bandwidth over two interfering links. For example, consider two neighboring co-channel links i and j along a path. Links i and j have bandwidth B_i and B_j , respectively. Since the two links can not be active simultaneously, the equivalent *achievable bandwidth under the intra-flow interference* (ABIRF) over links i and j , denoted as $ABIRF(ij)$, satisfies

$$\frac{L}{ABIRF(ij)} = \frac{L}{B_i} + \frac{L}{B_j} \quad (10)$$

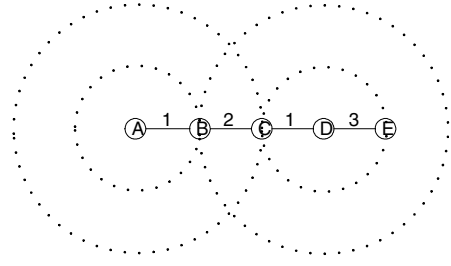


Fig. 2. Illustration of a multi-radio multi-channel path.

where L denotes the packet length. It can then be obtained that

$$ABIRF(ij) = \frac{B_i B_j}{B_i + B_j}. \quad (11)$$

Extending the $ABIRF(ij)$ result to the whole sub-path can be iteratively implemented. In each iteration, consider those links having been processed as one virtual link, with the bandwidth set as the ABIRF value already obtained; and then apply the computation of (11) over the virtual link and the next-hop link. Note that the impact of inter-flow interference on path capacity can be conveniently integrated with the intra-flow interference impact by using the ABITF value given by (9) as link capacity in ABIRF computation, instead of using the physical bandwidth.

3) *Multi-radio achievable bandwidth*: The multi-radio multi-channel connection makes the capacity analysis of a sub-path more complicated. When two links work on different channels through different radio interfaces, they could send/receive packets simultaneously without interference. It is possible that the two end-hops of a sub-path are co-channel links, while other hops in the middle may work on different channels. The iterative procedure discussed above to compute the ABIRF for a co-channel sub-path can also be extended to the multi-channel sub-path, with consideration that the achievable bandwidth over two links is $\min(B_i, B_j)$, when link i and j work over different channels. Specifically, the iterative steps to compute the ABIRF for a given multi-radio sub-path is as follows:

Step 1: For the first link of the sub-path, set $ABIRF$ equal to the ABITF associated with the channel over which the link works.

Step 2: Go to the next link, say link i , and check whether the channel of the next link is different from those used by the previous links or not. If different, go to step 3; otherwise go to step 4.

Step 3: In this case, set

$$ABIRF = \min(ABIRF, ABITF_i) \quad (12)$$

and then go to step 5.

Step 4: In this case, set

$$ABIRF = \frac{ABIRF \times ABITF_i}{ABIRF + ABITF_i} \quad (13)$$

and then go to step 5.

Step 5 : Check whether all the $(r + 2)$ hops of the sub-path have been considered or not. If not, go to step 2; otherwise, terminate the iteration.

For a H -hop path including multiple sub-paths, let $ABIRF_j$ denote the achievable bandwidth over the j th sub-path. The multi-radio achievable bandwidth can be computed as:

$$MRAB = \min (ABIRF_j) \quad (14)$$

for $j = 1, 2, \dots, H - r - 1$. If $H - r - 1 \leq 0$, we set $j = 1$, which means the path is so short that there is only one sub-path along the whole path. The computation in (14) exploits the bottleneck concept, but is applied at the sub-path level instead of the link level.

C. WEED Metric

1) *Weighted end-to-end delay*: Over a multi-radio multi-channel path, the MRAB metric is integrated with the EED metric to form a *weighted end-to-end delay metric* as:

$$WEED = \alpha \times \sum_{i=1}^H EED_i + (1 - \alpha) \times \frac{N_P \cdot L}{MRAB} \quad (15)$$

where $0 \leq \alpha \leq 1$ is tunable weight factor. In the WEED metric, the first part represents the accumulation of the delivery delay due to hop-by-hop transmissions in a store-and-forward manner; the second part represents the extra delay due to the interference nature of a multi-hop wireless network. In particular, the N_P induced in (15) denotes the total number of packets queued in the buffers along the path, because the interference effect described by the MRAB applies to all the packets that are being served by the path.

We would like to emphasize that the WEED metric contains not only the end-to-end delay information regarding a single packet transmission, but also the transmission delay for a block of packets due to the bottleneck bandwidth MRAB. Therefore, selecting a shortest path based on the WEED metric tends to minimize both the short-term and the long-term delay.

2) *Monotonicity analysis*: It has been indicated in [11] that monotonicity is one of the necessary properties of a routing metric to result in a consistent and loop-free routing implementation. For example, the well-known WCETT metric [13] is monotonic. We here prove that WEED also has the property of monotonicity.

Consider a given path, it is obvious that the $\sum_{i=1}^H EED_i$ part will become larger when one more hop is attached to the path. For the MRAB part, one more hop may lead to two possible cases. In the first case, the number of sub-paths does not change; the new hop just makes the $(H - r - 1)$ th sub-path one hop longer. According to the iterative computation given in Section IV-B, the ABIRF of a sub-path is less than or equal to the previous value when one more hop is included. Thus, the $\frac{N_P \cdot L}{MRAB}$ part achieves a larger/equal value when the path goes longer. In the second case, a new sub-path is incurred by the new hop, while the existing sub-paths will not change. The “minimization” operation in obtaining

the MRAB value guarantees that MRAB will not increase when one more sub-path is generated. Hence, $\frac{N_P \cdot L}{MRAB}$ part achieves a larger or equal value too in the second case, when one hop is involved. Since both parts constituting the WEED metric become larger or maintain equal when the path goes longer, WEED is monotonic. The proof applies to both left-monotonicity and right-monotonicity.

D. Channel Diversity Coefficient

A challenging issue being widely studied in the area of multi-channel wireless networks is how to quantify the channel diversity for a given path. Intuitively, an ideal quantity describing the channel diversity incorporates the impacts from various aspects, including the number of hops, the number of channels, and the interference relationship among the links. Our development efforts in the above have demonstrated that the MRAB metric indeed takes all of the factors into account. Therefore, we define a *channel diversity coefficient* (CDC) based on the MRAB as

$$CDC = \frac{MRAB}{B_s} \quad (16)$$

where B_s denotes the achievable bandwidth of the same path if all links of this path work over the same channel, defined as the *single-channel path capacity*. For the convenience of comparison, we adopt the smallest $ABITF_i$ value as the single-channel path capacity B_s . Thus, CDC is always larger than or equal to 1, and a higher CDC indicates a better channel diversity.

V. ROUTING PROTOCOL DESIGN

A. Basic DSR Implementation

We implement the proposed EED/WEED based routing by modifying the dynamic source routing (DSR) protocol [12]. We select DSR due to the following reasons: (i) DSR is one of the most popular protocols in multi-hop wireless networks, and the implementation codes are publicly available. (ii) We have noticed that some well-known routing metrics, such as ETX, ETT and WCETT, are implemented based on DSR; a common implementation will significantly facilitate the performance comparison among different routing metrics. (iii) The EED/WEED metric does not have the property of isotonicity [11], so the source routing approach (adopted by DSR) is preferred to guarantee the optimality, consistency, and loop-freeness in routing.

With basic DSR, a node attempts to find a route to a given destination by initiating a *route request* (RREQ) message. Every RREQ has a unique broadcast ID to prevent routing loops and redundant flooding. An intermediate node will further broadcast a RREQ only when the broadcast ID appears for the first time; also the node will insert its address in the source route field of the RREQ message. Once the destination receives the RREQ, it will reverse the hop sequence of the received path and insert the reversed path into the source route field of a *route reply* (RREP) message, which is then unicasted back to the source node. The source node will determine a

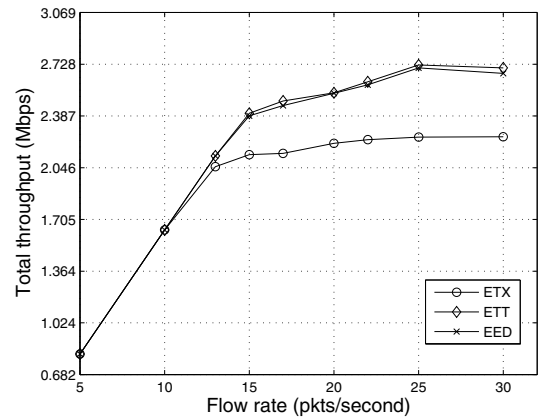
shortest path to a destination based on the path information it receives from the RREP messages. With DSR, all the RREP messages and data packets carry a complete path between a certain source/destination pair in their source route fields. All the nodes can overhear such path information and store it in their route caches for later use. In cases that a node finds that a packet could not be successfully delivered over a link after a maximum number of retransmission, the node will return a *route error* (RRER) to the source node of the path; every intermediate node receiving the RRER message will mark this link invalid.

B. EED/WEED Based Routing

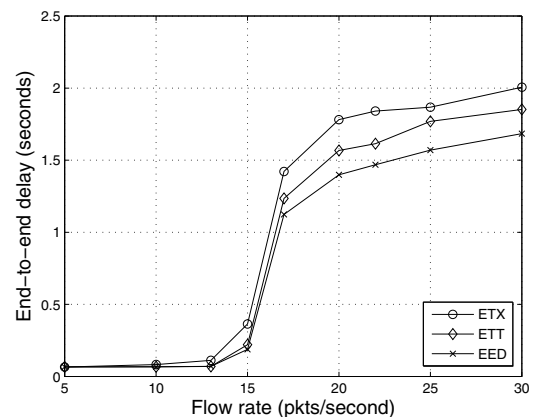
1) *EED link metric*: The EED metric itself can be used as a routing metric, especially for single-channel multi-hop networks. We consider that a directional link is defined by an upstream end and a downstream end, and the communication between two neighbor nodes is through two directional links. To obtain the EED link metric, a downstream node needs to monitor the transmission failure probability over the link and knows the number of packets in the upstream node's buffer. In our routing protocol, each node periodically broadcasts probe packets to its downstream neighbors at a predetermined rate λ , with the number of packets M in its buffer carried in each probe. Each downstream node maintains a neighbor list. When the downstream node receives a probe packet, it will update the value M for the corresponding upstream node in its neighbor list. Moreover, a downstream node will count the number of probes received from each upstream node during a period T ; use V_i to denote the number of probes received from the upstream node associated with link i . The transmission failure probability over link i can be estimated as $p_i = \frac{V_i}{\lambda T}$. The p_i value will also be stored into the neighbor list. After a downstream node finishes processing a received probe packet, the probe will be discarded.

A new field, called *link metric* is established in the RREQ message to store the metric value of each link. Once a node receives a RREQ, it first checks its own neighbor list to get the values of M_i and p_i , and then computes the EED according to (5). The metric EED_i will be inserted into the RREQ message if the node needs to continuously forward it. In addition, every node collects the EED metrics carried in the RREQ or RREP messages and store them in a *link cache*. The cached link metrics can be used to establish a network topology. If a node has a packet for a destination with the path information not established yet, the node can apply the Dijkstra's algorithm to compute an EED based shortest path based on the link cache information.

2) *WEED over a multi-radio path*: To implement the WEED based routing, each radio interface in the network is uniquely identified with a separate IP address for each interface. By considering each interface as the entity involved in the routing, the operations of probing, maintaining neighbor list and link cache, estimating the transmission failure probability are similar to the node based case. There is an additional field in all control messages to denote which interface is processing



(a) Total network throughput



(b) Average end-to-end delay

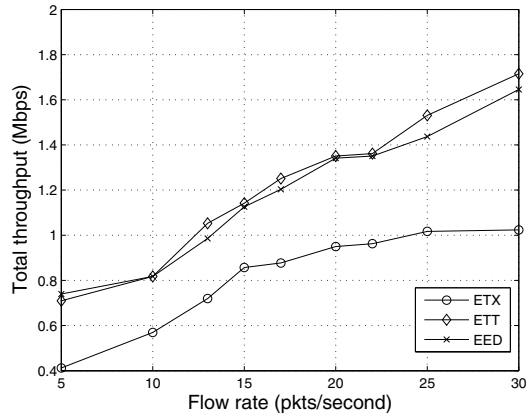
Fig. 3. The routing performance in grid topology versus flow rate.

the message. To calculate the MRAB of each sub-path, two extra fields need to be added to each record in the neighbor list: the channel ID indicating the channel associated with a link, and the IDR value computed according to (8) based on power monitoring at the downstream node. When a node forwards a RREQ message, the channel ID, the IDR values, and EED all are attached as link metrics. Once the destination receives the RREQ, it will return a RREP to the source node, which duplicates all the routing information retrieved from the RREQ. Based on the RREP messages, the source can finally compute a shortest path regarding the WEED metric, according to (15).

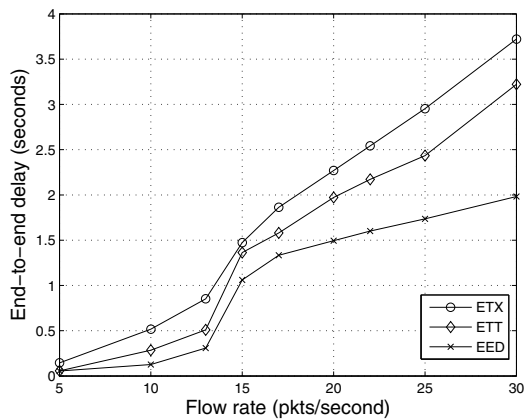
VI. PERFORMANCE EVALUATION

A. EED-Based Routing in a Single-Channel Network

The EED metric by itself can be used as an efficient routing metric, since it effectively captures not only the queuing delay at the network layer but also the retransmission delay at the MAC layer. We use NS2 simulation results for a single-channel wireless mesh network to demonstrate the performance, with comparison with the two well-know metrics ETX and ETT. The MAC protocol used for simulation is 802.11b.



(a) Total network throughput

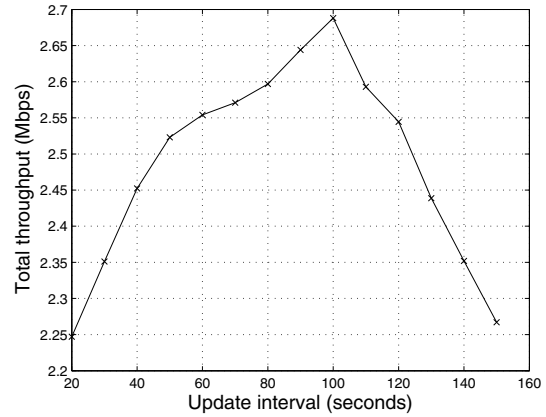


(b) Average end-to-end delay

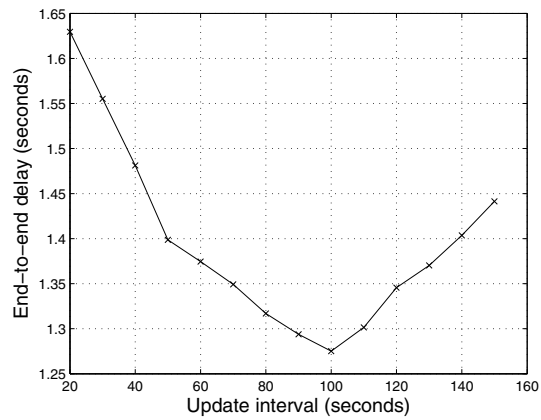
Fig. 4. The routing performance in random topology versus flow rate.

We specifically consider two network topologies. The first is a grid topology over a $1400m \times 1400m$ area. The area is divided into $200m \times 200m$ square cells, with each cell containing one network node in its center. Four flows are deployed at the 1st, 3rd, 5th, and 7th rows of the grid, respectively, with the source/destination nodes of each flow located at both ends of the row correspondingly. The other topology randomly places 40 nodes in a $1000m \times 1000m$ area with necessary adjustment to maintain the connectivity. We also run 4 flows over the random topology. For both topologies, the transmission range is 250m, and the interference range is 550m. All flows are constant-bit-rate (CBR) flow, with the packet size of 512 bytes.

Fig. 3 and Fig. 4 present the total network throughput and end-to-end delay, under ETX, ETT, and EED metrics, respectively, versus the flow rate. The queue size at each node is 20 packets, and the link metric update interval in our EED implementation is 50 seconds. In the two figures, it is explicitly demonstrated that EED metric can result in much better end-to-end delay performance than ETX and ETT, under both the grid and random topologies. Regarding the network throughput, ETT and EED has the similar performance, while outperforming the ETX. The reason that ETT and EED have similar throughput performance is that both of them exploit the



(a) Total network throughput

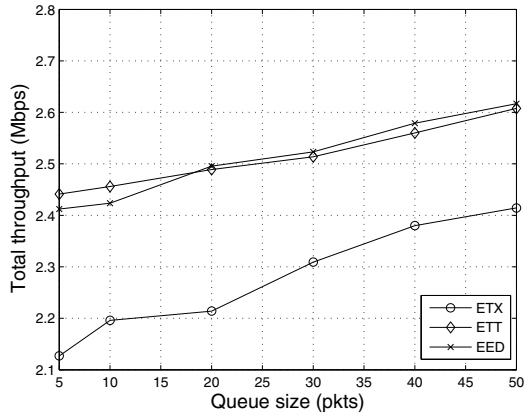


(b) Average end-to-end delay

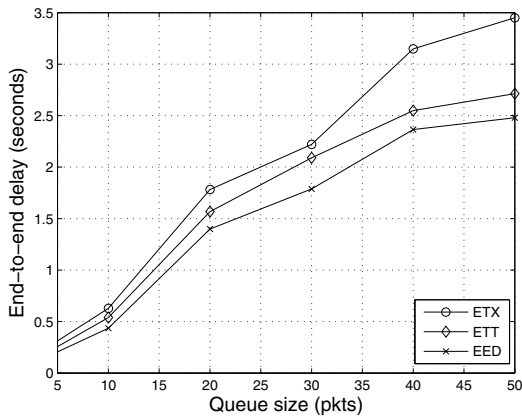
Fig. 5. The impact of EED update interval on routing performance.

transmission failure probability for computing the link metric, while the transmission failure probability is directly related to the MAC throughput [7]. In most of the cases, ETT has slightly higher throughput, which is due to the larger computation overhead with EED and implementation overhead due to path change incurred by the random queue length behavior. In addition, we observe in the grid topology that the throughput curves under all the three metrics become flat when the flow rate exceeds a certain level, which indicates that the network is approaching its maximum capacity.

We next examine the impact of EED update interval on the routing performance. The grid topology is simulated, with the queue size at each node being 20 packets and flow rate 25 packets/second. Fig. 5(a) and 5(b) present the network throughput and the end-to-end delay versus the EED updating interval, respectively. From the figure, it can be seen that both inappropriate small and large intervals result in low throughput and large delay. On one hand, an inappropriate small update interval induces over-frequent link metric update and results in a large bandwidth overhead. On the other hand, an inappropriate large update interval will not timely respond to a congested link and result in unnecessary packet loss due to a full buffer. Fig. 5 demonstrates that an optimal update



(a) Total network throughput



(b) Average end-to-end delay

Fig. 6. The impact of queue size on routing performance.

interval exists that can lead to largest throughput and smallest end-to-end delay.

We further evaluate the effect of queue size on the routing performance, with results illustrated in Fig. 6. The grid topology is considered with the EED update interval of 50 seconds and the flow rate of 20 packets/second. Regarding the throughput as shown in Fig. 6(a), we can see that ETT performance better for small buffer sizes, while EED better for large ones. The reason is that when the buffer size is small, in most of the cases all the buffers are full, where the EED could not exploit more benefit compared to the ETT. The extra computation overhead and route updating overhead, however, will lead to a smaller network throughput. When the buffer is large, EED can select a path with more buffer space, which will lead to less tail-dropping of the packets and thus a higher throughput. Regarding the delay as shown in Fig. 6(a), EED achieves the smallest end-to-end delay in all the cases.

B. Metric Comparison in Multi-channel Environment

In this part, we use an example to illustrate the effectiveness of WEED in quantifying the capacity of a multi-radio multi-channel path. Since there is no much reference on NS2 simulation of DSR-based routing over multi-radio wireless networks, we are still developing such a NS2 simulation

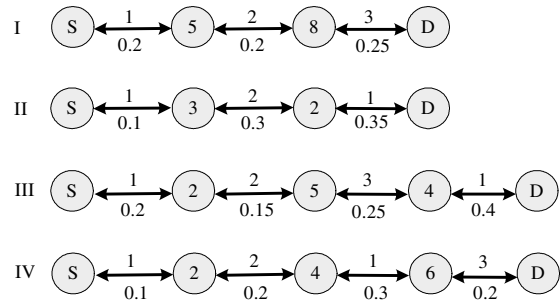


Fig. 7. WEED and WCETT Examples.

TABLE I
PARAMETERS USED IN NUMERICAL ANALYSIS

| Parameters | Values |
|-------------------------------|-----------|
| Packet length | 600 bytes |
| Link bandwidth over channel 1 | 8 Mbps |
| Link bandwidth over channel 2 | 12 Mbps |
| Link bandwidth over channel 3 | 6 Mbps |
| Minimum contention window | 0.02 ms |
| Maximum retransmission times | 5 |

package. Thus, we resort to numerical analysis here to obtain the results.

The path selection example is shown in Fig.7, where the interference range $r = 1$ hop. There are four candidate paths with three possible channels. The numbers within each circle indicate the number of packets waiting in the buffer of that node. The channel assignment is marked above the link, and the transmission failure probability below. Other necessary parameters for WEED computation are illustrated in Table I. For the convenience of analysis, we ignore the power monitoring part for inter-flow interference analysis, while the intra-flow interference analysis here is sufficient for demonstrating the capability of WEED in quantifying the channel diversity.

We compare the path selection based on WEED and WCETT, with results shown in Table II and III. WCETT prefers path I over II, and IV over III, while WEED prefers the other way. By investigating the configuration of Path I and II, it is obvious that WEED makes a different decision from WCETT's because it takes the number of packets in the buffers into consideration. The advantage of WEED over WCETT can be demonstrated by comparing path III with path IV. Since the two interfering links over channel 1 are located further away in path III than in path IV, it is intuitively clear that path III suffers a less amount of intra-flow interference. Moreover, both path III and path IV consist of the same set of links (two channel-1 links, one channel-2, one channel-3), so path III will achieve a higher path capacity than path IV due to the less interference over it. Thus, WCETT makes a wrong decision, while WEED makes a correct one. The reason for WCETT's wrong decision is that it deems that co-channel links along a path always interfere with each other, disregard the distance among them. With $r = 1$, it is obvious that the two channel-1 links in path III will not interfere with each other, in fact.

TABLE II
NUMERICAL RESULTS FOR WCETT [13]

| Path | $\sum_{i=1}^H ETT_i$ | $\max(X_j)$ | WCETT ($\beta = 0.5$) |
|------|----------------------|-------------|-------------------------|
| I | 2.3881 | 1.0667 | 1.7274 |
| II | 2.1612 | 1.5898 | 1.8755 |
| III | 3.2873 | 1.75 | 2.5187 |
| IV | 3.0238 | 1.5238 | 2.2738 |

TABLE III
NUMERICAL RESULTS FOR WEED

| Path | $\sum_{i=1}^H EED_i$ | MRAB | WEED ($\alpha = 0.5$) | CDC |
|------|----------------------|---------|-------------------------|--------|
| I | 16.6991 | 6Mbit/s | 13.5496 | 3.0 |
| II | 5.8638 | 4Mbit/s | 5.9319 | 2.0 |
| III | 13.8753 | 6Mbit/s | 11.33765 | 4.0 |
| IV | 13.6927 | 4Mbit/s | 14.04635 | 2.6667 |

Table III illustrates that the MRAB and CDC value can quantitatively demonstrate the capacity difference between two multi-radio multi-channel paths. Moreover, the MRAB and CDC values also reveals the interesting insight that the relationship between the channel diversity and the length of the path in terms of hop count is not monotonic. For example, path III achieves better channel diversity than path I, being one-hop longer; but path I has better channel diversity than path IV, being one-hop shorter.

VII. CONCLUSION

In this paper, we aims at designing link/path metrics that can lead to path selection with the minimum end-to-end delay, while a high network throughput can also be achieved. The paper has key contributions in two aspects: 1) Based on the concept of network/MAC cross-layer design, both the queuing delay in network layer and transmission delay in the network layer are included in the EED link metric computation; 2) A generic iterative approach is developed to compute the achievable bandwidth over a multi-radio multi-channel path, which captures the complex interaction among hop count, channel assignment, and inter/intra flow interferences to form the WEED path metric. A side benefit of our EED/WEED link metric computation is a quantitative channel diversity coefficient. We demonstrate the performance of EED/WEED based routing via extensive numerical analysis and NS2 simulation results.

REFERENCES

[1] P. Gupta and P. R. Kumar, "The capacity of wireless networks," *IEEE Trans. Inform. Theory*, vol. 46, no. 2, pp. 388–404, Mar. 2000.

[2] M. Gastpar and M. Vetterli, "On the capacity of wireless networks: the relaycase," in *Proc. IEEE INFOCOM*, 2002, pp. 1577–1586.

[3] A. E. Gamal, J. Mammen, B. Prabhakar, and D. Shah, "Throughput-delay trade-off in wireless networks," in *Proc. IEEE INFOCOM*, 2004, pp. 464–475.

[4] I. F. Akyildiz, X. Wang, and W. Wang, "Wireless mesh networks: a survey," *Computer Networks*, 2005, pp. 523–530.

[5] G. Jakllari, S. Eidenbenz, N. Hengartner, S. V. Krishnamurthy, and M. Faloutsos, "Link Positions Matter: A Noncommutative Routing Metric for Wireless Mesh Network," in *Proc. IEEE INFOCOM*, 2008, pp.744–752.

[6] C. Koksai and H. Balakrishnan, "Quality-Aware Routing Metrics for Time-Varying Wireless Mesh Networks," *IEEE J. Select. Areas Commun.*, vol. 24, no.11, pp. 1984–1994, November.2006.

[7] Y. Cheng, X. Ling, W. Song, L.X. Cai, W. Zhuang, and X. Shen "A Cross-Layer Approach for WLAN Voice Capacity Planning," *IEEE J. Select. Areas Commun.*, vol. 25, no. 4, pp. 678–688, May 2007.

[8] A. Raniwala, T.-c. Chiueh, "Architecture and Algorithms for an IEEE 802.11-Based Multi-Channel Wireless Mesh Network," in *Proc. IEEE INFOCOM*, 2005, pp. 2223–2234.

[9] A.Cerpa, J. L. Wong, M. Potkonjak and D. Estrin, "Temporal Properties of Low Power Wireless Links: Modeling and Implications on Multi-Hop Routing," in *Proc. ACM MobiHoc*, 2005, pp. 414–425.

[10] K. N. Ramachandran, E. M. Belding, K. C. Almeroth and M. M. Buddhikot, "Interference-Aware Channel Assignment in Multi-Radio Wireless Mesh Networks," in *Proc. IEEE INFOCOM*, 2006, pp.1-12.

[11] Y. Yang, J. Wang, "Design Guidelines for Routing Metrics in Multihop Wireless Networks," in *Proc. IEEE INFOCOM*, 2008, pp.1615 - 1623.

[12] D. B. Johnson, D. A. Maltz and Y. Hu, "The Dynamic Source Routing Protocol for Mobile Ad Hoc Networks (DSR)," in *IETF, INTERNET-DRAFT*, 2003, April.

[13] R. Draves, J. Padhye, and B. Zill, "Routing in Multi-Radio, Multi-Hop Wireless Mesh Networks," in *ACM MOBICOM*, 2004, pp. 114–128.

[14] R. Draves, J. Padhye, and B. Zill, "Comparison of Routing Metrics for Static Multi-Hop Wireless Networks," in *ACM SIGCOMM*, 2004, pp. 133–144.

[15] Y. Yang, J. Wang, and R. Kravets, "Designing Routing Metrics for Mesh Networks," in *Proc. IEEE Workshop on Wireless Mesh Networks (WiMesh)*, 2005.

[16] J. So, N. H. Vaidya, "Load-Balancing Routing in Multichannel Hybrid Wireless Networks With Single Network Interface," in *IEEE Trans. Veh. Technol.*, vol. 56, no. 1, pp. 342–348, Jan. 2007.

[17] T. Liu, W. Liao, "Capacity-Aware Routing in Multi-Channel Multi-Rate Wireless Mesh Networks," in *Proc. IEEE ICC*, 2006, pp. 1971–1976.

[18] K. Jain, J. Padhye, V. N. Padmanabhan, and L. Qiu, "Impact of Interference on Multi-hop Wireless Network Performance," in *ACM MOBICOM*, 2003, pp. 66–80.

[19] X. Li, H. Chen, Y. Shu and X.Chu, "Energy Efficient Routing With Unreliable Links in Wireless Networks," in *Proc. IEEE International Conference on Mobile Adhoc and Sensor Systems (MASS)*, 2006, pp. 160–169.

[20] H. Zhai, Y. Fang "Impact of Routing Metrics on Path Capacity in Multi-rate and Multi-hop Wireless Ad Hoc Networks," in *Proc. IEEE ICNP*, 2007, pp. 86–95.

[21] D. S. J. De Couto, D. Aguayo, J. Bicket, and R. Morris, "A High-Throughput Path Metric for Multi-Hop Wireless Routing," in *ACM MOBICOM*, 2003, pp. 134–142.

[22] K. Kim, K. G. Shin, "On accurate measurement of link quality in multi-hop wireless mesh networks," in *ACM MOBICOM*, 2006, pp. 38–49.

[23] H. Zhai, J. Wang and Y. Fang, "Distributed packet scheduling for multihop flows in ad hoc networks," in *Proc. IEEE WCNC*, 2004, pp. 1081–1086.

[24] Y. Xiao, K. Thulasiraman and G. Xue, "QoS routing in communication networks: approximation algorithms based on the primal simplex method of linear programming," in *IEEE Trans. Comput.*, vol. 55, no. 7, pp. 815–829, July. 2006.

[25] H. Li, Y. Cheng, C. Zhou, "Multi-hop effective bandwidth based routing in multi-radio wireless mesh networks," in *Proc. IEEE Globecom*, 2008.

[26] J. Tang, G. Xue, and W. Zhang, "Interference-Aware Topology Control and QoS Routing in Multi-Channel Wireless Mesh Networks," in *ACM MobiHoc*, 2005, pp. 68–77.

[27] The Network Simulator - NS2, <http://www.isi.edu/nsnam/ns/>.

[28] "Wireless Lan Medium Access Control (MAC) and Physical Layer (PHY) specifications," ANSI/IEEE Std 802.11: 1999 (E) Part 11, ISO/IEC 8802-11, 1999.

[29] A. Raniwala, T.-c. Chiueh, "Centralized Channel Assignment and Routing Algorithms for Multi-Channel Wireless Mesh Networks," in *ACM SIGMOBILE Mobile Computing and Communications Review*, 2004, pp. 50–65.

[30] A. Abdrabou and W. Zhuang, "Service time approximation in IEEE 802.11 single-hop ad hoc networks," *IEEE Trans. Wireless Commun.*, vol. 7, no. 1, pp. 305-313, Jan. 2008.